28–39 GHz Distributed Harmonic Generation on a Soliton Nonlinear Transmission Line

Eric Carman, Kirk Giboney, Michael Case, Masayuki Kamegawa, Ruai Yu, Kathryn Abe, M. J. W. Rodwell, and Jeff Franklin

Abstract—**A second-harmonic generation is reported in the 26–40 GHz band through soliton propagation on a GaAs monolithic nonlinear transmission line. At 20 dBm input power, a 20-diode structure attained < 12 dB conversion loss for input frequencies from 13.5–18 GHz, with 9.3 dB minimum conversion loss, while a 10-diode structure attained < 12 dB loss, 14–19.5 GHz (7.3 dB minimum). With reduction of conductor skin losses, broadband operation and peak conversion efficiencies approaching −3 dB are attainable.**

SCHOTTKY diode frequency multipliers driven by phase-locked microwave generators are low phase-noise millimeter-wave signal sources widely used in receivers and instrumentation. Using Schottky diodes as nonlinear conductances, high conversion efficiencies are not attainable, while lumped-element Schottky varactor diode multipliers have reactive input and output impedances which cannot be matched efficiently over a broad bandwidth.

Harmonic generation can also be performed on periodic nonlinear transmission lines (NLTL's) [1]–[5], structures having periodically distributed nonlinear capacitance. Monolithic GaAs NLTL's have generated step-functions with ~ 1.3 ps falltimes [6, 7] through shock generation [8], while chirped-periodic GaAs NLTL's [9] have generated 5.5 ps impulses through soliton propagation [10]. Through soliton propagation on periodic NLTL's, harmonic generation with broad bandwidth and high efficiency is feasible. Here we report millimeter-wave frequency multiplication using soliton propagation on a periodic monolithic NLTL. In contrast to the work of Marsland *et al.* [1], we have attained higher conversion efficiency and broad bandwidth.

A periodic NLTL is a ladder network of high impedance line sections loaded at constant intervals with reverse-biased diodes serving as voltage-variable capacitors (Fig. 1(a)). If the diodes have capacitance $C_d(V)$, the interconnecting high-impedance line sections have characteristic impedance Z_L and electrical delay τ, and if $C_d(V) \gg \tau/Z_L$, then the structure can be approximately modelled as an LC ladder network having $L = Z_L\tau$ and $C(V) = C_d(V) + \tau/Z_L$ (Fig. 1(b)). The diodes have a parasitic series resistance r_d.

The small-signal propagation constant on the periodic structure is $\beta(\omega) = \cos^{-1}(1 - 2(\omega/\omega_b)^2)$, where $\omega_b = 2/\sqrt{LC(V_{\text{bias}})}$ is the Bragg frequency. The small-signal characteristic impedance is $Z_0(\omega) = V_n(\omega)/I_n(\omega) = \sqrt{L/C(V_{\text{bias}})}\sqrt{1 - (\omega/\omega_b)^2} + j\omega L/2$; both the per-section phase delay $T_p(\omega) = \beta/\omega$ and Z_0 show strong variation at frequencies approaching ω_b.

With a large signal input voltage V_{in}, the voltage variation of the NLTL capacitance results in nonlinear wave propagation, and harmonics of the input frequency ω_1 are generated. In NLTL's here the Bragg frequency ω_b is much larger than ω_1, shock waves with transition times of the order of $1/\omega_b$ [6]–[8] are generated, and power is generated in many harmonics of ω_1. Hence, efficient conversion of the input power to a single desired harmonic is not attained.

Harmonics at frequencies higher than ω_b do not propagate; if $\omega_b < 3\omega_1$, generation of the third and higher order harmonics is suppressed, and the conversion efficiency to the second harmonic is enhanced, as shown by analyses by Jäger [3]. The resulting distributed second harmonic generation, governed by both the nonlinear capacitance and periodic network dispersion, can be described either in terms of the propagation of sets of solitons [11], [12], or in terms of propagation of the fundamental and second harmonic coupled by the diode voltage-variable capacitance [2], [3], [5].

NLTL second-harmonic generation can be described in terms of large-signal nonlinear propagation, and the resulting generation of sets of solitons [11], [12]. If $C(V) = C_0/(1 - V/V_0)$ (V negative), the LC ladder network supports the propagation of solitons of the form [12]

$$V_n(t) = -V_{\max}\,\text{sech}^2\big(1.212(t - nT_D)/T_{FWHM}\big), \quad (1)$$

where the propagation delay

$$T_D = \sqrt{LC_0V_0/V_{\max}}\,\sinh^{-1}\big(\sqrt{V_{\max}/V_0}\big), \quad (2)$$

and the soliton pulse width

$$T_{FWHM} = 1.212\sqrt{LC_0V_0/V_{\max}} \quad (3)$$

are functions of the soliton amplitude $V_{\max}$. For given L, C_0, and V_0, the soliton amplitude $V_{\max}$ has a unique corresponding full-width at half maximum impulse width T_{FWHM} and per-section propagation delay T_D. For solitons with amplitude $V_{\max} \simeq V_0$, (3) is approximated by $T_{FWHM} \sim \pi/\omega_b$.

Impulses of amplitude $V_{\max}$ having duration $T_{FWHM} > 1.212\sqrt{LC_0V_0/V_{\max}}$ correspond to a nonlinear superposition of a set of solitons having differing amplitudes $V_{\max}$ and differing propagation delays T_D; applied to the NLTL, such a pulse will decompose into this set of two or more solitons during propagation [12]. A sinusoidal input at frequency ω_1 corresponds to a repetitive train of negative-going input impulses of

Manuscript received October 15, 1990; revised November 6, 1990. This work was supported by the Air Force Office of Scientific Research under Grant AFOSR-89-0394.

E. Carman, K. Giboney, M. Case, R. Yu, K. Abe and M. J. W. Rodwell are with the Department of Electrical and Computer Engineering, University of California, Santa Barbara, CA 93106.

M. Kamegawa is on leave from Shimadzu Corporation, Kyoto, Japan. He is with the Department of Electrical and Computer Engineering, University of California, Santa Barbara, CA 93106.

J. Franklin is with Varian Associates III–V Device Center, Santa Clara, CA 95054.

IEEE Log Number 9041824.

1051-8207/91/0200-0028$01.00

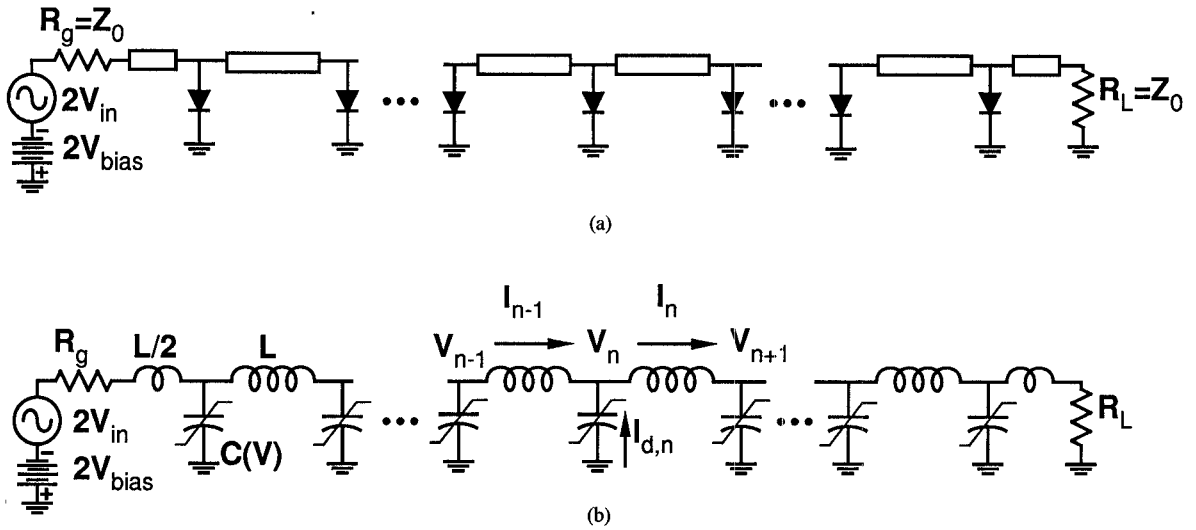

Fig. 1. (a) Nonlinear transmission line circuit diagram, and (b) L-C ladder network equivalent circuit.

duration $T_{FWHM} = \pi/\omega_1$, each corresponding to a superposition of a set of solitons which subsequently separate during propagation.

Experimentally, using direct electrooptic sampling [13], we observe the decomposition of sinusoidal inputs into sets of solitons (Fig. 2) on a 20-diode monolithic NLTL with $\omega_b = 2\pi(44)$ GHz. Each negative cycle of a 15 GHz, 20 dBm input decomposes into a pair of negative-going pulses which progressively separate during propagation. The output shows two distinct pulses per cycle, and a strong second harmonic component. With further propagation on a longer NLTL, the lower-amplitude soliton of a given input cycle merges with the larger-amplitude soliton of the subsequent input cycle, and the second-harmonic power decreases. Pulses much longer than $2\pi/\omega_b$ separate into progressively larger numbers of solitons; a 10 GHz input (Fig. 2) decomposes into sets of 3 solitons per cycle, and a strong output third harmonic is generated. Efficient 2nd harmonic generation occurs for $\omega_b/3 < \omega_1 < \omega_b/2$.

Described instead in terms of coupled propagation of Fourier components, harmonics of ω_1 are generated by the voltage-variable capacitance. Assume that $C(V) \simeq C_0 + C_1(V - V_{bias})$ and that the voltage V_n at the nth diode has Fourier components at the fundamental ω_1 and the second harmonic $\omega_2 = 2\omega_1$, $V_n(t) = V_{bias} + V_{n1}\cos(\omega_1 t + \phi_1) + V_{n2}\cos(\omega_2 t + \phi_2)$. The nonlinear capacitance term C_1 generates currents at ω_2 of $I_{d,n}^{\omega 1 \to \omega 2} = (C_1\omega_1 V_{n1}^2/2)\sin(\omega_2 t + 2\phi_1)$, at ω_1 of $I_{d,n}^{\omega 1, \omega 2 \to \omega 1} = (C_1\omega_1 V_{n1}V_{n2}/2)\sin(\omega_1 t + \phi_2 - \phi_1)$, and at higher harmonics of ω_1.

Neglecting higher harmonics (nonpropagating if above ω_b), these currents will cause the fundamental to exchange power with the second harmonic, which in the case of phase-matched fundamental and second harmonic [3]–[5], will generate a second harmonic wave whose amplitude grows with propagation distance. Solution of the coupled propagation equations is beyond the scope of this letter (see [2]–[5]). The second harmonic amplitude reaches a maximum after a distance of $n_{max} \simeq \pi/\omega_2 |T_p(\omega_2) - T_p(\omega_1)|$. With further propagation, the phase angle between the accumulated second harmonic wave amplitude and the second harmonic conversion current $I_{d,n}^{\omega 1 \to \omega 2}$ exceeds $\pi/2$, and the second harmonic amplitude decreases.

The coupled-harmonic model again predicts peak conversion efficiency for $\omega_b/3 < \omega_1 < \omega_b/2$. At higher input frequencies,

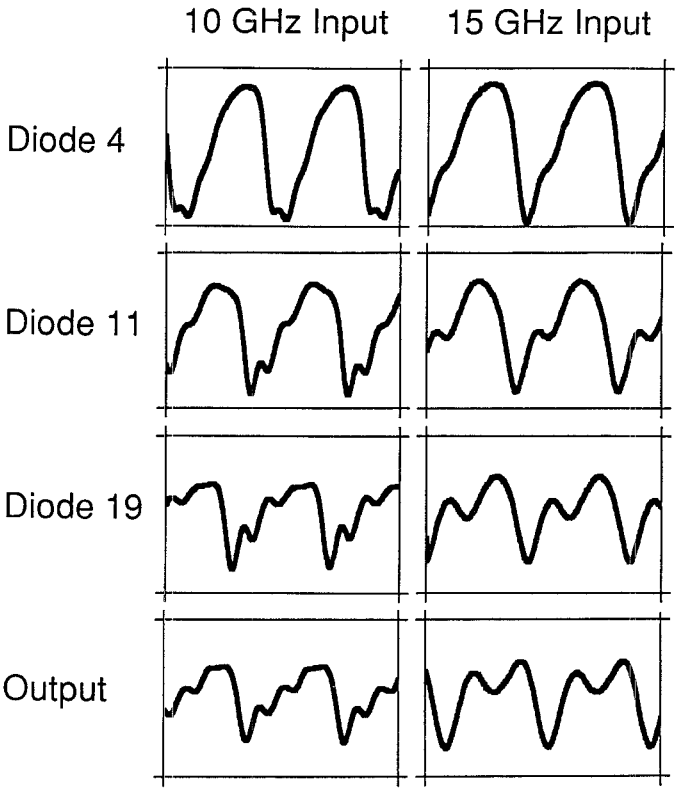

Fig. 2. Experimentally observed waveforms illustrating soliton decomposition in 20-diode NLTL with 44 GHz Bragg frequency. Input is 20 dBm sine wave with −2.6 V bias.

the second harmonic cannot propagate, while at lower input frequencies, $3\omega_1 < \omega_b$, the third harmonic can propagate, and parasitic third harmonic generation occurs. To maximize conversion efficiency, the number of NLTL sections is selected to be approximately n_{max} in the center of this passband, approximately 20 diodes. Jäger [3] and Champlin [5] give solutions to the coupled harmonic model given the cases where either the phase mismatch $|T_p(\omega_2) - T_p(\omega_1)|$ is negligible, or the depletion of the fundamental power with propagation is negligible. Because neither assumption holds for our devices, we predict the conversion loss (second harmonic output power divided by fundamental input power) using standard circuit analysis simula-

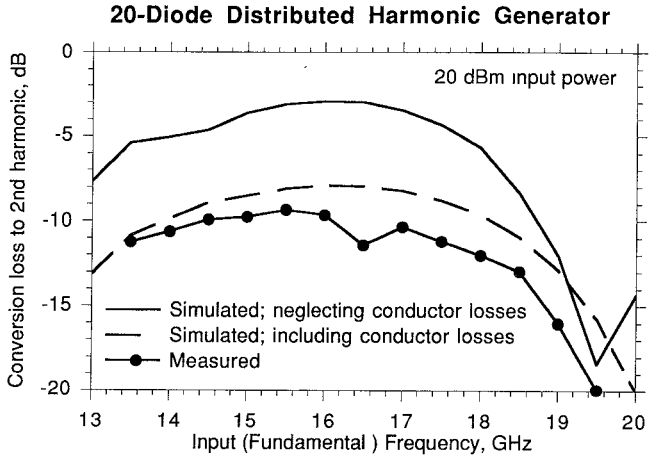

Fig. 3. Simulated and measured conversion loss in second harmonic generation: 20-diode NLTL with 20 dBm input and −2.6 V bias.

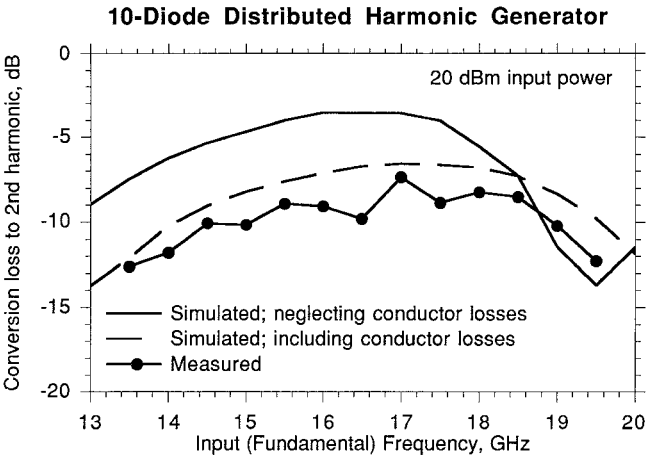

Fig. 4. Simulated and measured conversion loss in second harmonic generation: 10-diode NLTL with 20 dBm input and −2.4 V bias.

tion software (SPICE and a harmonic-balance circuit simulator [14]).

10-diode and 20-diode NLTL distributed harmonic generators were fabricated using processes similar to those of refs. [6], [7]. Schottky diodes are formed on a GaAs semiinsulating substrate with a exponentially graded 425 nm thickness N^- active layer whose doping variation with depth is $N^-(d) = N_0 \exp(-d/d_0)$ where d is the distance from the wafer surface, $N_0 = 2 \times 10^{17}/\text{cm}^3$ and $d_0 = 225$ nm. A buried 1 μm thick N^+ layer ($6 \times 10^{18}/\text{cm}^3$ doping, 7 Ω per square sheet resistivity) provides the diode cathode connections. Ohmic contacts to the N^+ layer (with 0.02 Ω-mm resistivity) are formed by a 0.5 μm $NH_4OH/H_2O_2/H_2O$ recess etch, a self aligned AuGe-Ni-Au liftoff, and a rapid thermal anneal. Proton implantation using both 180 kev, $1.7 \times 10^{15}/\text{cm}^2$ and 100 kev, $4 \times 10^{14}/\text{cm}^2$, provides > 50 MΩ per square isolation, defining diode contact areas and eliminating N^+ and N^- layer conductivitier near the coplanar-waveguide sections, reducing dielectric losses. During implantation, a 1.7 μm Au-10 μm polyimide mask protects ohmic contacts and diode active regions. The transmission lines are formed with a 800 Å Ti-80 Å Pt-11000 Å Au liftoff; Schottky contacts result where the Ti-Pt-Au liftoff intersects the unimplanted N-layer. At 3 μm design rules, the diodes have an ~ 800 GHz zero-bias cutoff frequency $f_{d,0} = 1/2\pi C_d(0) r_d$.

For the 20-diode NLTLs, $Z_L = 90$ Ω, $\tau = 4$ ps, and $C_d(V) \simeq C_{j0}/(1 - V/\phi)^M$, where $C_{j0} = 247$ fF, $\phi = 1$ Volt, and $M = 0.708$. At $V_{\text{bias}} = -2.6$ V, $\omega_b = 2\pi(44)$ GHz, and $Z_0(\omega = 0) = 50$ Ω, while the parameters (least-square-error) fitted to the Hirota [12] soliton model are $L = 0.36$ nH, $C_0 = 274$ fF, and $V_0 = 3.2$ V. The 10-diode NLTL has $\tau = 4.4$ ps, $C_{j0} = 272$ fF, $C_0 = 301$ fF, and $\omega_b = 2\pi(40)$ GHz at $V_{\text{bias}} = -2.4$ V. Neglecting skin-effect losses, circuit simulations predict 3 dB conversion loss at peak efficiency, and < 6 dB loss 13.2-18.1 GHz for the 20 diode structures; 3.5 dB minimum conversion loss is predicted for the 10-diode NLTLs.

Conversion efficiency for the monolithic devices was measured on-wafer using a synthesized microwave source and a 26-40 GHz spectrum analyzer, whose calibrations were verified with a precision power meter, and DC-40 GHz bias tees and wafer probes, whose losses were determined using a network analyzer. Experimental results are compared with harmonic-balance circuit simulations [14]. With 20 dBm input power at −2.6 V bias, the 20-diode NLTL attains 9.3 dB insertion loss at peak efficiency and 13.5-18 GHz bandwidth at < 12 dB loss (Fig. 3), while the 10-diode NLTL (−2.4 V bias) attains 7.35 dB minimum insertion loss and 14-19.5 GHz bandwidth at < 12 dB loss (Fig. 4). The lower-than-predicted conversion loss arises from skin-effect losses on the 90 Ω interconnecting line sections (1.4 μm thick gold with 10 μm line width, giving a calculated attenuation of $47.4 \times \sqrt{f/1\ \text{GHz}}$ dB/m), which have relatively low Q. When these skin losses are modelled, measured conversion loss is ~ 2 dB greater than simulation. The 10 diode lines are shorter than $n_{\max}$ but attain higher efficiency through reduced skin losses. Circuit implementation with planar spiral inductors or lower-impedance line sections will reduce metallic losses, permitting conversion loss to approach the theoretical −3 dB.

In summary, we have demonstrated millimeter-wave distributed frequency multiplication on a monolithic GaAs device. The circuits are directly scalable to millimeter-wave frequencies beyond 100 GHz. With use of lower-loss inductive elements, broad bandwidth, high efficiency millimeter-wave frequency multiplication will be feasible.

Acknowledgment

We acknowledge the assistance of John Bowers with electrooptic sampling.

References

[1] R. A. Marsland, M. S. Shakouri, and D. M. Bloom, "Millimeter-wave generation on a nonlinear transmission line," *Electron. Lett.*, vol. 26, no. 16, pp. 1235-1236, Aug. 2, 1990.

[2] A. Scott, *Active and Nonlinear Wave Propagation in Electronics*. New York: Wiley-Interscience, 1970.

[3] D. Jäger and F.-J. Tegude, "Nonlinear wave propagation along periodic-loaded transmission line," *Appl. Phys.*, vol. 15, pp. 393-397, 1978.

[4] D. Jäger, "Characteristics of travelling waves along nonlinear transmission lines for monolithic circuits: A review," *Int. J. Electron.*, vol. 58, no. 4, pp. 649-669, 1985.

[5] K. S. Champlin and D. R. Singh, "Small-signal second-harmonic generation by a nonlinear transmission line," *IEEE Trans. Microwave Theory Tech.*, vol. MTT-34, no. 3, pp. 351-353, Mar. 1986.

[6] C. J. Madden, R. A. Marsland, M. J. W. Rodwell, D. M. Bloom, and Y. C. Pao, "Hyperabrupt-doped GaAs nonlinear transmission line for pi cosecond shock-wave generation," *Appl. Phys. Lett.*, vol. 54, no. 11, pp. 1019-1021, Mar. 13, 1989.

[7] R. Y. Yu, M. Case, M. Kamegawa, M. Sundaram, M. J. W. Rodwell, and A. W. Gossard, "275 GHz 3-mask integrated GaAs sampling circuit," *Electron. Lett.*, vol. 26, no. 13, pp. 949-951, June 21, 1990.

[8] R. Landauer, "Shock waves in nonlinear transmission lines and their effect on parametric amplification," *IBM J. Res. and Dev.*, vol. 4, no. 4, pp. 391–401, Oct. 1960.

[9] M. Case, M. Kamegawa, R. Y. Yu, K. Giboney, M. J. W. Rodwell, J. Bowers, and J. Franklin; "62.5 ps to 5.5 ps Soliton Compression on a monolithic nonlinear transmission line," *1990 Device Res. Conf.*, Postdeadline paper, Santa Barbara, CA, June 25–27, 1990.

[10] M. Tan, C. Y. Su, and W. J. Anklam, "7 × electrical pulse compression on an inhomogeneous nonlinear transmission line," *Electron. Lett.*, vol. 24, no. 4, pp. 213–215, Feb. 1988.

[11] A. C. Scott, F. Y. F. Chu, and D. W. McLaughlin, "The soliton, a new concept in applied science," *Proc. IEEE*, vol. 61, no. 10, pp. 1443–1482, Oct. 1973.

[12] R. Hirota and K. Suzuki, "Theoretical and experimental studies of lattice solitons in nonlinear lumped networks," *Proc. IEEE*, vol. 61, no. 10, pp. 1483–1491, Oct. 1973.

[13] K. J Weingarten, M. J. W. Rodwell, and D. M. Bloom, "Picosecond sampling of GaAs integrated circuits," *IEEE J. Quantum Electron.*, vol. 24, no. 2, pp. 198–220, Feb. 1988.

[14] LIBRA and Microwave SPICE, EEsof, Inc., 5795 Lindero Canyon Road, Westlake Village, CA, 91362.